Combined Concurrent Photodynamic and Gold Nanoshell Loaded Macrophage-Mediated Photothermal Therapies: An *In Vitro* Study on Squamous Cell Head and Neck Carcinoma

Anthony J. Trinidad, BA,[1]* **Seok Jin Hong,** MD,[1,2] **Qian Peng,** MD, PhD,[3] **Steen J. Madsen,** PhD,[4] and **Henry Hirschberg,** MD, PhD[1,4]

[1]*Beckman Laser Institute and Medical Clinic, University of California, Irvine, California 92612*

[2]*Department of Otorhinolaryngology-Head and Neck Surgery, Kangbuk Samsung Hospital, Sungkyunkwan University School of Medicine, Seoul, Korea*

[3]*Pathology Clinic, Rikshospitalet-Radiumhospitalet HF Medical Center, University of Oslo, Montebello, Oslo N-0310, Norway*

[4]*Department of Health Physics and Diagnostic Sciences, University of Nevada, Las Vegas, Nevada 89154*

Background and Objective: Treatment modalities, such as hyperthermia and photodynamic therapy (PDT) have been used in the treatment of a variety of head and neck squamous cell carcinoma (HNSCC), either alone or as an adjuvant therapy. Macrophages loaded with gold nanoshells, which convert near-infrared light to heat, can be used as transport vectors for photothermal hyperthermia of tumors. The purpose of this study was to investigate the effects of combined macrophage mediated photothermal therapy (PTT) and PDT on HNSCC cells.
Study Design/Materials and Methods: Gold nanoshell loaded rat macrophages either alone or combined with human FaDu squamous cells in hybrid monolayers were subjected to PTT, PDT, or a simultaneous combination of the two light treatments. Therapies were given concurrently employing two laser light sources of $\lambda = 670$ nm (PDT) and $\lambda = 810$ nm (PTT), respectively.
Results: Significant uptake of gold nanospheres (AuNS) by rat alveolar macrophages was observed thus providing the rationale for their use as delivery vectors. Viability of the AuNS-loaded Ma was reduced to 35 and 12% of control values at an irradiance of 14 or 28 W/cm^2 administered over a 5 minute period respectively. No significant cytotoxicity was observed for empty Ma for similar PTT exposure. AlPcS$_{2a}$ mediated PDT at a fluence level of 0.25 J/cm^2 and PTT at 14 W/cm^2 irradiance had little effect on cell viability for the FaDu/Ma (ratio 2:1) hybrid monolayers. In contrast, combined treatment reduced the cell viability to less than 40% at these same laser power settings.
Conclusions: The results of this study provide proof of concept for the use of macrophages as a delivery vector of AuNS for photothermal enhancement of the effects of PDT on squamous cell carcinoma. A significant synergy was demonstrated with combined PDT and PTT compared to each modality applied separately. Lasers Surg. Med. © 2014 Wiley Periodicals, Inc.

Key words: combinatorial PDT & PTT; gold nanoshells; HNSCC; hyperthermia; macrophage; PDT; PTT; photothermal therapy; photodynamic therapy; squamous cell carcinoma

INTRODUCTION

Head and neck squamous cell carcinoma (HNSCC) is the most common type of malignant tumor in the upper aerodigestive tract. Standard therapy for HNSCC is surgical resection followed by a combination of radiation and chemotherapy to eliminate remaining tumor cells or metastases. Despite advancements in imaging and surgical techniques to achieve organ preservation, there has been little improvement in survival rates over the past 50 years [1].

Treatment modalities, such as hyperthermia (HT) and photodynamic therapy (PDT) have been used in the treatment of a variety of HNSCC, either alone or as an adjuvant therapy [2–8]. HT is a strong sensitizer of radiotherapy and a number of cytotoxic drugs. Many tumors recur after chemo-radiation due to the resistance of hypoxic cells to these forms of treatment. In contrast, hypoxic cells are susceptible to cell death following HT as this is an oxygen independent treatment [9]. HT induces cell death through mechanisms such as protein

denaturation and rupture of cellular membranes. Various sources for heat generation, including radiofrequency and microwaves, laser light, and ultrasound have been employed [10,11]. These direct methods, however, if not combined with an additional targeting moiety, cannot distinguish normal from tumor tissue, resulting in unwanted toxicity.

To increase the specificity of laser mediated hyperthermia, exogenous tumor-targeted heating agents such as dyes, silica–gold nanoshells (AuNS), or nanorods, have been used in a variety of *in vitro* and *in vivo* tumor models with promising results [12–16].

AuNS, are composed of a dielectric core (silica) coated with an ultrathin gold layer and can absorb or scatter light at NIR wavelengths, a light region in which optical penetration through tissue is optimal. Importantly, AuNS convert absorbed NIR to heat with an efficacy, and stability that far exceeds that of conventional dyes [17–19]. Activated by near infrared laser light (NIR) photothermal therapy (PTT) can provide specific heating of diseased regions while minimizing thermal insult to normal tissue.

One important criterion for nanoparticle-based therapy is the targeted delivery of the nanoparticles. Cell-based vectorization is one method that can target and maintain an elevated concentration of nanoparticles at the tumor site and prevent their spread into normal tissue [20–22]. Employing macrophages, in conjunction with nanoparticle delivery for PTT has interesting potential for cancer treatment since they are attracted to hypoxic and necrotic regions within tumors [23]. In a previous study, macrophages were employed as delivery vectors for AuNS into glioma spheroids for PTT [24].

Although NIR light penetrates moderately well in tumor tissue at depth, the effects of PTT will be suboptimal, allowing the survival of a population of cancer cells. Methods to increase the efficacy of PTT would therefore be of interest.

PDT of cancer involves the utilization of a tumor-localizing photosensitizing agent that, upon activation by light, results in the destruction of neoplastic tissue by direct tumor ablation, tumor-vasculature damage, and immune response activation [25–28]. PDT has also been used on a variety of head and neck cancers with promising results [8]. We and others have previously shown that the efficacy of PDT can be increased by moderate externally induced hyperthermia [29–32]. Additionally, the effects of various types of dual-function nano-systems for synergistic PDT and PTT have been explored [33–36].

Since both HT and PDT have been tested clinically for the treatment of HNSCC, the possibility of a synergistic effect of combining these treatment forms prompted the present study. In the experiments reported here, we have examined the effects of AuNS-loaded Ma mediated PTT and PDT, separately and in combination on HNSCC cell monolayers. Two different wavelengths of light were employed simultaneously, one to activate a highly efficient PDT photosensitizer (670 nm) and the other for the AuNS-Ma PTT (810 nm) to evaluate the combined effects of these modalities.

MATERIALS AND METHODS

Cell Lines

The human FaDu cancer cell line (ATCC, HTB-43) and rat alveolar Ma (NR8383; ATCC# CRL-2192), were both obtained from the American Type Culture Collection (Manassas, VA), The cells were cultured in Dulbecco's Modified Eagle Media (DMEM, Gibco, Carlsbad, CA) with high glucose and supplemented with 2 mM L-glutamine, gentamycin (100 mg/ml), and 2% heat-inactivated fetal bovine serum (Gibco) at 37°C in a 7.5% CO_2 incubator.

Nanoshells

The gold nanoshells (AuNS) used in this study consisted of a 120 nm silica core with a 12–15 nm gold shell (Nanospectra Biosciences, Inc., Houston, TX). The resultant optical absorption peak was between $\lambda = 790$ and 820 nm for PEGylated particles. The absorbance curves of PEGylated nanoshell solutions were supplied by the manufacturer. The solutions were found to have an optical density (OD) of 1.22 at $\lambda = 795$ nm for PEGylated nanoshells (100× dilution).

Ma-AuNS Incubation

NR8383 rat alveolar Ma were seeded in 35 mm cell culture dishes at 1×10^6 Ma in 2 ml of culture medium. The dishes were incubated overnight to allow the cells to settle and adhere to the plastic. Culture medium was exchanged for 100 µl of PEGylated (2.8×10^{11} particles/ml) nanoshells colloid in 1.9 ml of culture medium. The Ma were incubated for 24 hours at 37°C, rinsed three times with Hanks' Balanced Salt Solution with calcium chloride and magnesium chloride (HBSS, Gibco) to wash away the excess of non-ingested nanoshells. AuNS laden Ma (designated Ma^{NS}) were then detached with trypsin, and a rubber spatula washed and counted. The concentration of nanoshells in macrophages was studied using a UV–Vis-NIR spectrophotometer (Varian UV–Vis-NIR spectrophotometer Cary 6000i, Varian, USA).

Absorbance was measured at a spectrum involving $\lambda = 600–1,100$ nm wavelengths, which covers the broad absorption peak of nanoshells ($\lambda = 819$ nm).

PTT or PDT Only Treatment

All light treatment was performed at a culture temperature of 37°C. For PTT only treatment, eight wells in a vertical column in 96-well ultra low adhesion round-bottomed plates (Corning, Inc., Corning, NY) were seeded with either Ma, Ma^{NS}, or FaDu + Ma^{NS} cells at a total density of 5×10^3 cells per well. The plates were centrifuged at 1,000g for 10 minutes to force the cells into a small disk at the bottom of the well and incubated for 24 hours prior to experimentation. Cells were plated into every fourth column (eight wells) in order to minimize the contribution of light scatter to the non-treated cultures. For PTT, individual wells were irradiated with $\lambda = 810$ nm laser light (Coherent, Inc., Santa Clara, CA) at irradiances ranging from 0 to 14 W/cm^2 with a beam diameter of
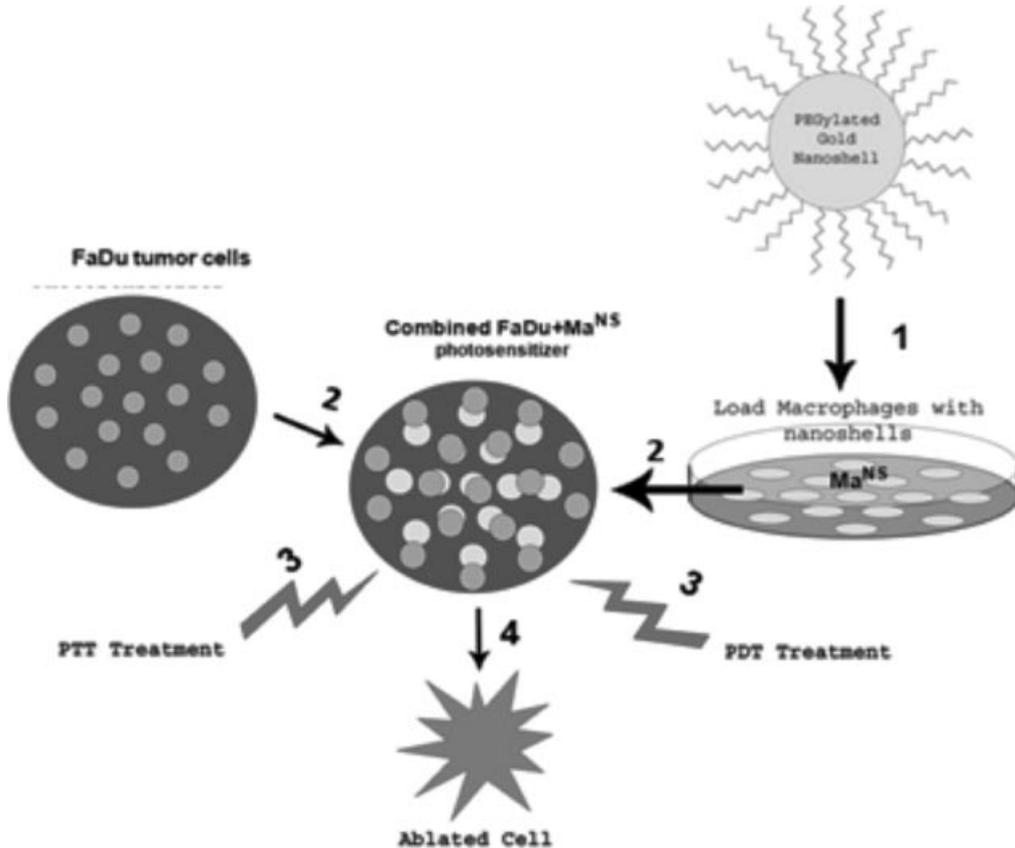
Fig. 1. **Basic concept of combined AuNS-Ma mediated PTT and PDT 1**. Rat NR8383 Ma incubated with AuNS for 24 hours. 2. FaDu tumor cells combined with AuNS Ma (Ma[NS]) together with photosensitizer AlPcS2a 24 hours. 3. Concurrent laser irradiation @ 670 nm (PDT) and 810 nm (PTT) 5–10 minutes. 4. Cell death.

approximately 3 mm. Laser exposure times of either 5 or 10 minutes were used.

For PDT only treatment, FaDu + Ma[NS] cells were incubated with 1 µg/ml of the photosensitizer AlPcS$_{2a}$ (Frontier Scientific, Inc., Logan, UT) and DMEM for 18 hours and washed three times. 5×10^3 cells were aliquoted into each well (every fourth column of 8 wells) as previously explained. Irradiation was done using $\lambda = 670$ nm light from a diode laser (Intense, North Brunswick, NJ). The cells were exposed to a range of radiant exposures (0.15–0.75 J/cm^2) delivered for 5 minutes at light irradiances that varied from 0.5 to 2.5 mW/cm^2 through an opaque mask that allowed illumination of one column of eight wells at a time. Following either PTT or PDT laser irradiance, incubation was continued for 48 hours, at which point the culture medium was replaced with fresh clear buffer containing MTS (3-(4,5-dimethylthiazol-2-yl)-5-(3-carboxymethoxyphenyl)-2-(4-sulfophenyl)-2H-tetrazolium MTS, Promega, Madison, WI) reagents and incubated for an additional 2 hours. The OD was measured using an ELx800 uv Universal Microplate Reader (Bio-Tek Instruments, Inc., Winooski, VT).

Combined PDT–PTT Treatment

Figure 1 shows the set-up for two wavelength light treatment. FaDu and Ma[NS] were combined at a ratio of FaDu:Ma[NS] of 2:1. 100 µl of medium containing 5×10^3 cells were aliquoted into the wells of ultralow adherence round-bottomed plates and the plates centrifuged at 1,000g for 10 minutes as previously described. AlPcS$_{2a}$ (1 µl/ml) was added to each well, and the plates incubated for 18 hours. The cells were washed three times to remove excess photosensitizer. Individual wells were irradiated with 810, 670 nm or a combination of the two wavelengths. Six hundred seventy nano meter irradiation both alone and combined was performed through an opaque mask that allowed only one well at a time to be treated. For combined treatment, the wells were irradiated simultaneously, 670 nm from above, 810 from below. Following laser irradiance, incubation was continued for 48 hours and cell survival was assayed by MTS assay as previously described. The degree of synergism was calculated for combined PTT–PDT treatments compared to PTT or PDT alone. The equation shown below was used to determine if the combined effect was synergistic, antagonistic, or
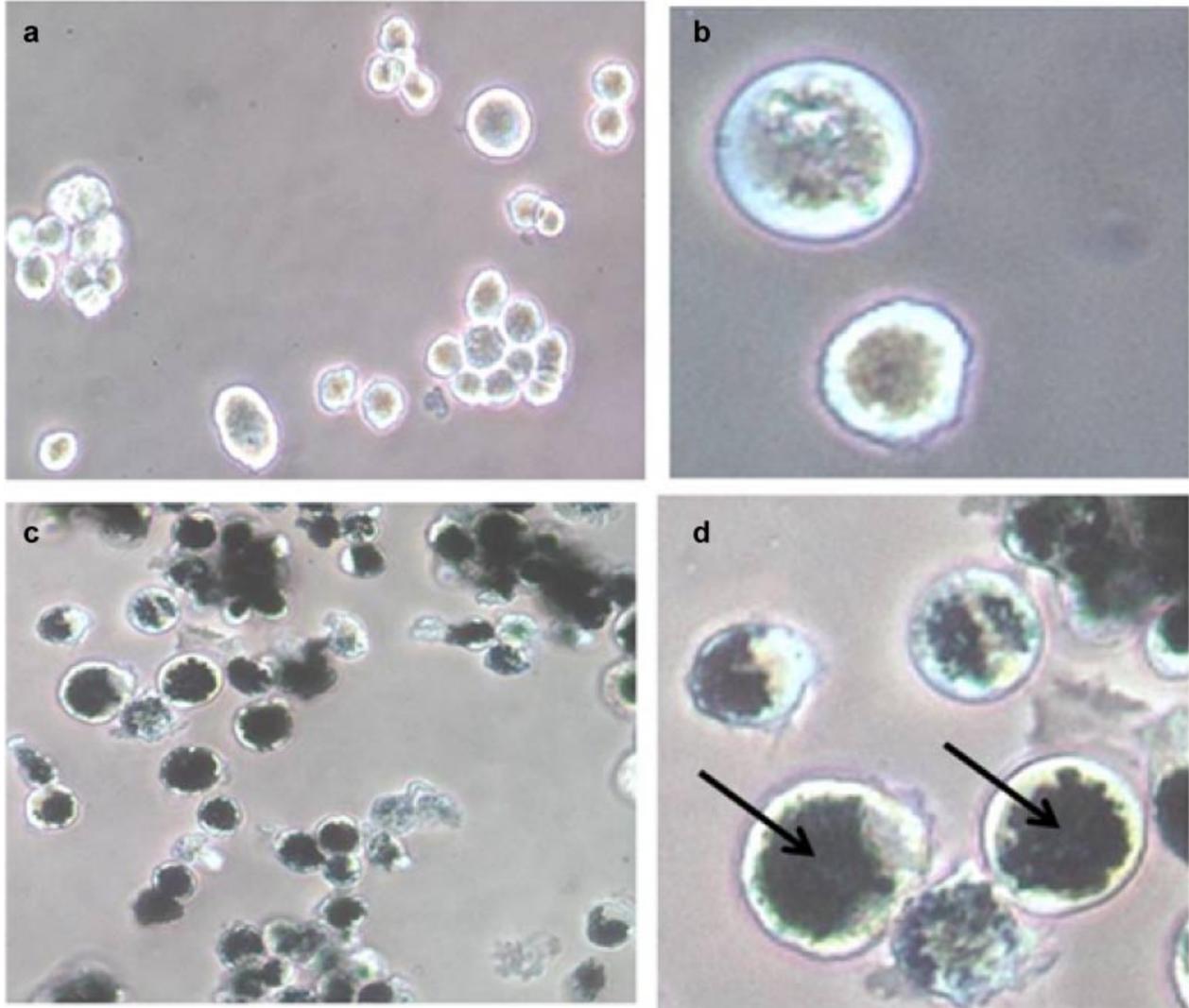
Fig. 2. Phase-contrast micrographs of non-loaded (**a** and **b**) and AuNS-loaded rat alveolar macrophages (**c** and **d**). Macrophages were incubated with AuNS for 24 hours. The AuNS appear as dark, opaque regions in c and d (arrow in d). A magnification of $10\times$ was used for a and c, while b and d are magnified by $40\times$. (AuNS; Gold nanoshell).

additive, where "α" is the ratio of the cumulative effect of two therapies administered independently to the net effect of combining the two therapies at a given dose.

$$\alpha = \frac{\left(\mathrm{SF}^{\mathrm{a}} \times \mathrm{SF}^{\mathrm{b}}\right)}{\mathrm{SF}^{\mathrm{a}}}$$

In this scheme SF^{i} represents the survival fraction for a specific treatment. If $\alpha > 1$, the result is synergistic (supra-additive). If $\alpha < 1$, the result is antagonistic, and if $\alpha = 1$ the result is simply additive [20].

Statistical Analysis

Microsoft Excel was employed for the calculation of the arithmetic mean, standard deviation, and standard error. Experimental data were analyzed using one-way ANalysis Of VAriance (ANOVA) at the significance level of $P < 0.05$ and presented as mean with standard error unless otherwise noted.

RESULTS

Macrophage Endocytosis of Bare or PEGylated Nanoshells

The strategy of employing *in vitro* loading of macrophage vectors would dictate a maximum uptake of nanoparticles by the macrophages. It was therefore of interest to determine the ability of the rat alveolar macrophages used in this study to take up PEGylated nanoshells compared to bare Ma. The percent uptake of PEGylated nanoshells in the macrophages was lower (10%) than that of bare nanoshells (36%). However, the PEGylated nano-shell solution was available at a much higher concentra-tion since they have a much lower tendency to aggregate
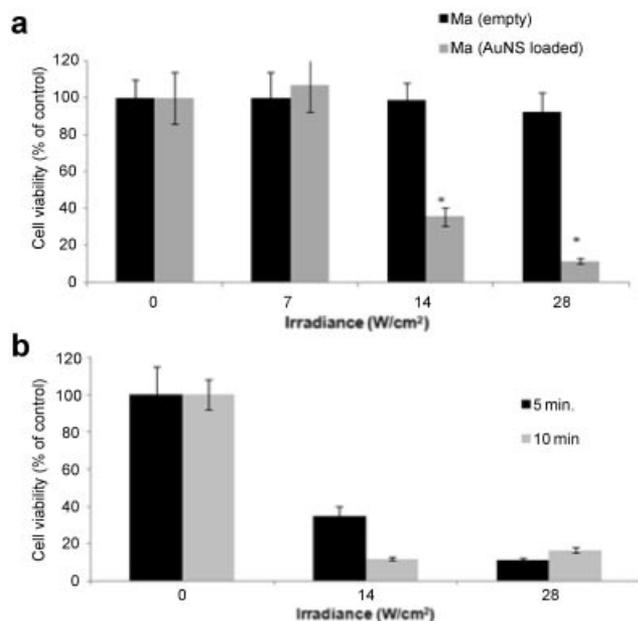
Fig. 3. PTT on empty Ma and AuNS-loaded Ma (Ma^{NS}) monolayers. (**a**) Effects of laser power on cell viability. 5×10^3 Ma or Ma^{NS} in the wells of round bottomed 96 well-plate were exposed to NIR laser powers of 0, 7, 14, and $28 \, W/cm^2$ for 5 minutes. MTS viability assay was done 24 hours later. Each data point represents the mean ($\pm SE$) of eight replicate cultures/trial, in two independent experiments. (**b**) The effect of NIR exposure time. Ma^{NS} were exposed to NIR irradiance of 14 or $28 \, W/cm^2$ for 5 or 10 minutes. Each data point represents the mean ($\pm SE$) of eight replicate cultures/trial, in two independent experiments.

compared to bare nanoshells. 1×10^6 Ma incorporated 30×10^8 PEGylated nanoshells versus 3.5×10^8 bare nanoshells. PEGylated nanoshells were therefore used in all subsequent experiments. The internalized NS in Ma were visualized as dark opaque regions in phase-contrast microscopy images (Fig. 2c and d). These dark areas are absent in the control Ma, which were not incubated with NS (Fig. 2a and b).

PTT on AuNS Loaded MA (Ma^{NS})

Since it is the Ma^{NS} that convert the NIR laser energy into heat delivering hyperthermia to cancer cells, it was important to determine the effects of PTT on Ma and Ma^{NS} directly. 5×10^3 Ma or Ma^{NS} in the wells of round-bottomed 96-well plates were exposed to NIR laser powers of 0, 7, 14, and $28 \, W/cm^2$ delivered with a beam size of 3 mm in order to achieve the high radiant exposures necessary in a reasonable time period. The effects of NIR laser irradiation on empty and NS-loaded Ma are shown in Figure 3a. Viability of the NS-loaded Ma was reduced to 35 and 12% of control values at an irradiance of 14 or $28 \, W/cm^2$ administered over a 5 minutes period respectively. No significant cytotoxicity was observed for empty Ma even at irradiances of $28 \, W/cm^2$ for 5 minutes. The effect of NIR exposure time at two different irradiances is shown in Figure 3b. Comparing the cytotoxic effect of irradiating the cells at a laser power of $14 \, W/cm^2$ for 10 minutes to $28 \, W/$

cm^2 for 5 minutes showed no significant differences. This indicates that it was the total radiant exposure that was of importance.

PTT and PDT on FaDu–Ma^{NS} Cells

The effects of Ma^{NS}-mediated PTT on FaDu cells are illustrated in Figure 4a. FaDu and Ma^{NS} were combined at two different FaDu:Ma^{NS} ratios, 1:1 and 2:1. In all cases, the total combined cell numbers were approximately 5×10^3. As can be seen from the figure, a significant decline in cell viability with increasing irradiance was demonstrated. At a FaDu:Ma^{NS} ratio of 1:1 and $14 \, W/cm^2$ irradiance about 50% of the cells survived compared to 35% for the Ma^{NS} PTT treated cells (Fig. 3a). At an irradiance of $28 \, W/cm^2$, there was no difference between the PTT effects on 100% Ma^{NS} (Fig. 3a) and the FaDu:Ma^{NS} combined cells (Fig. 4a).

In order to determine the cytotoxic effects of combined PTT/PDT on FaDu cells, it is necessary to establish a suboptimal light PDT dose. 5×10^3 combined FaDu and Ma^{NS} cells were irradiated with $\lambda = 670 \, nm$ at increasing radiant exposures from 0.15 to $0.75 \, J/cm^2$ at irradiances that varied from 0.5 to $2.5 \, mW/cm^2$ (Fig. 4b) since the irradiation time was fixed at 5 minutes. Radiant exposures between 0.25 and $0.5 \, J/cm^2$ resulted in 95% and 60% cell survival respectively. Radiant exposures greater than $0.5 \, J/cm^2$ induced a cell survival of less than 50%, and therefore the addition of PTT would be difficult to ascertain. Irradiating either monolayers of FaDu or FaDu + empty Ma at $\lambda = 810 \, nm$ in the presence AlPcS$_{2a}$ at $14 \, W/cm^2$ produced no significant differences in cell viability compared to controls (data not shown).

Combined PTT–PDT on FaDu–Ma^{NS} Cells

The effects of combined PTT and PDT are shown in Figure 5a and b. PTT irradiance was varied from 0 to $28 \, W/cm^2$ (Fig. 5a) with irradiance duration of 5 minutes. Three different PDT (670 nm) radiant exposures were examined. The irradiance was varied to achieve the desired radiant exposure in the 5 minutes NIR PTT exposure. The FaDu:Ma^{NS} ratio was 2:1. As can be seen from the figure, a significant reduction in cell viability was achieved at $14 \, W/cm^2$, 810 nm laser irradiance and a PDT radiant exposure of $0.25 \, J/cm^2$ ($P < 0.05$). At lower PTT irradiances ($7 \, W/cm^2$), no significant increase in the cytotoxic effects of PTT with the addition of PDT was observed ($P > 0.1$). Experiments were also performed over a range of PDT radiant exposures (0–$0.75 \, J/cm^2$) at a PTT irradiance of $14 \, W/cm^2$ (Fig. 5b). At radiant exposures exceeding $0.25 \, J/cm^2$, no significant increase in the effects of PDT on cell viability was demonstrated.

Quantitative evaluation of simultaneous PTT and PDT, as determined from the degree of interaction (α), was calculated from the data shown in Figure 5b and are shown in Table 1. The α-values for the effects of combined treatment cytotoxicity for a PTT irradiance of $14 \, W/cm^2$ ranged from 1.83 ± 0.16 to 2.29 ± 0.26 for the cells that received PDT radiant exposures of 0.5 and $0.25 \, J/cm^2$, respectively, clearly indicating a synergistic effect.
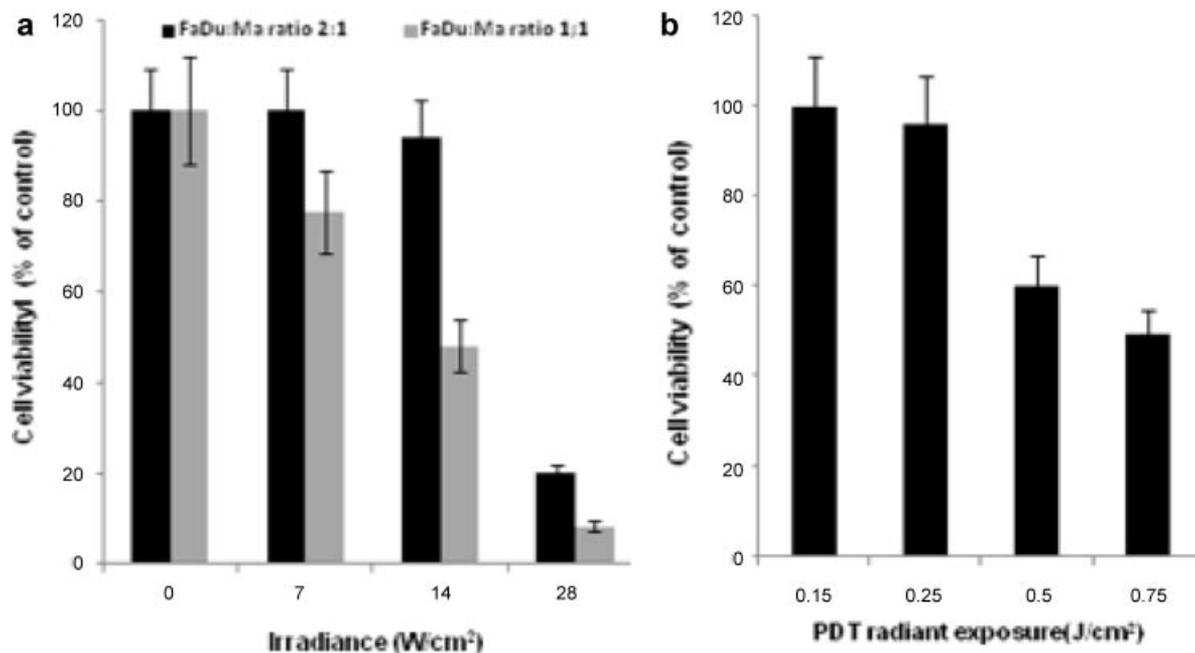
Fig. 4. Effects of either PTT or PDT treatment on combined FaDu–Ma^{NS} monolayers. (**a**) FaDu–Ma^{NS} monolayers at ratios of 1:1 or 2:1 for a total of 5×10^3 cells in each well of a round bottomed 96-well plate were irradiated with 810 nm light for 5 minutes per well at increasing laser power (0–28 W/cm^2). (**b**) Combined monolayers as described above were incubated for 18 hours with AlPcS2a, and were exposed to increasing 670 nm PDT irradiation (0–0.7 J/cm^2). PDT treatment was, in all cases, for a 5 minute duration. MTS assay was carried out 24 hours following treatment. Cell viability is shown as a percent value of untreated control cultures. Each data point represents the mean (±SE) of eight replicate cultures/trial, in two independent experiments.

DISCUSSION

Since head and neck tumors are often superficial, light activated therapies like PDT and PTT can be well suited for early stage HNSCC and in selected cases of diffuse disease. PDT has the advantage of reduced effect on connective tissues, healing with less scarring than after HT treatment, an improved cosmetic result and due to the low toxicity of most photosensitizers, treatment can be repeated.

The possibility of a synergistic effect between simultaneous PDT and PTT prompted the present study. PTT is an effective method of achieving rapid elevated temperatures in tissue in the presence of NIR absorbing AuNS while limiting damage to normal structures. The efficacy of PDT on tumor cells is enhanced by moderate hyperthermia and combined therapy has been shown to be effective [30–32]. Since HNSCC arise from a microenvironment rich in immune cells and these tumors have been found to contain significant quantities of macrophages, these tumors should therefore be good candidates for macrophage-mediated therapies. Stromal and tumor cells produce a wide spectrum of chemokines and growth factors able to recruit circulating monocytes and differentiate them into macrophages [37,38]. The ability of macrophages to migrate and accumulate within tumor tissue, including hypoxic regions, makes them attractive vehicles for the delivery of diagnostic or therapeutic agents such as nanoparticles. The most basic concepts of such a strategy involve the isolation of

monocytes from a given patient, which are differentiated *ex vivo* into macrophages, loaded with the agent of interest, and then reinjected into the patient [39,40].

Murine monocytes, loaded with AuNS, and exposed to NIR light, were shown in a previous publication to be highly effective at inducing growth inhibition of three dimensional glioma spheroids via hyperthermia, that is, PTT [24]. Compared to the murine monocytes employed in this latter study, the rat macrophages used here displayed a significantly increased ability to incorporate AuNS. Among the various polymers used to prevent NS removal from the circulation, polyethylene glycol (PEG) is currently the most popular and the most effective in prolonging circulation time of nanoparticles [41,42]. Nanoparticles are therefore often PEGylated to prevent their rapid elimination from the circulation by the reticuloendothelial system and to inhibit their propensity to aggregate. As shown in Figure 2, despite the PEGylation of AuNS, they are rapidly and effectively taken up by macrophages. This is in agreement with the findings of Yang et al. [43] where rat peritoneal macrophages were used with similar AuNS to those used here.

The goal of PTT is to induce heating in the tumor while minimizing thermal diffusion to surrounding tissues. Cytotoxic effects have been demonstrated in cells maintained at 42°C for 1 hour, and this duration can be shortened to 5–10 minutes by using higher temperatures of 46–50°C. This is clearly illustrated in Figure 3b where
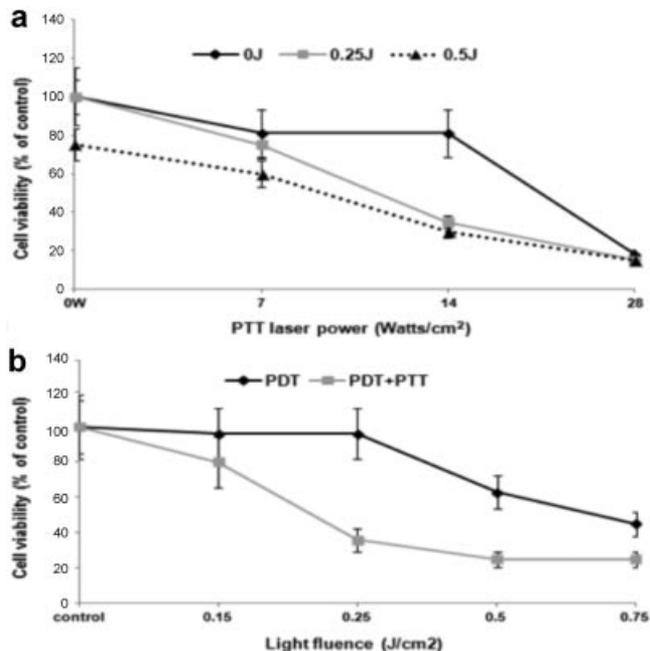
Fig. 5. Effects of concurrent PTT + PDT on combined FaDu–Ma[NS] monolayers. (**a**) FaDu–Ma[NS] monolayers at a ratio of 2:1 were exposed to 810 nm NIR light for 5 minutes at an increasing PTT irradiance from 0 to 28 W/cm². Three different PDT (670 nm) radiant exposures were examined. (**b**) 670 nm irradiation at a fixed PTT power of 14 W/cm² was varied from 0 to 0.75 J/cm². Treatment time was in all cases 5 minutes. PTT laser power ranged from 0.5 mW/cm² (0.15 J/cm²) to 2.5 mW/cm² (0.75 J/cm²). MTS assay was performed 48 hours after treatment. Each data point represents the mean (±SE) of eight replicate cultures/trial, in three independent experiments.

increasing the exposure time from 5 to 10 minutes gave the same PTT effect as increasing the laser power by a factor of 2. This indicates that the total radiant exposure (i.e., final cell temperature) was of importance. At the molecular level, hyperthermic effects can be seen as changes to the cytoskeletal structure, cell membrane rupture, protein denaturation, impairment of DNA and RNA synthesis, and apoptosis [44].

The minimum temperature increase for effective PTT ranges from 46 to 60°C, but higher temperature elevations may be required in hypoxic, low pH environments characteristic of many tumors [45]. PTT efficacy depends on a number of factors, including light distributions in tissues. Since NIR penetration depths in normal and malignant tissue are relatively modest (ca. 0.5–1.0 cm) effective PTT may require direct light delivery using optical fibers. Other factors affecting PTT efficacy include the distribution and concentration of nanoparticles in and near the tumor, which should be optimized so as to produce temperatures sufficient for effective hyperthermia. One of the main advantages of PTT is that hypoxic cells, found in the center of tumors, are susceptible to cell death following hyperthermia since the treatment is oxygen independent. In contrast, tumors recur after chemo-radiation and most probably PDT due to the survival of hypoxic cells, following these forms of treatment. Ma are known to be attracted to hypoxic regions of tumors so their use as cellular vectors for PTT inducing nanoparticles is therefore a logical choice.

The *in vitro* data presented in Figures 3 and 4a demonstrate that significant NIR induced PTT-cell death can be achieved in cancer cells in close contact with AuNS-loaded Ma, albeit at relatively high radiant exposures (14–28 W/cm²). These results are in qualitative agreement with those of Bernardi et al. [46], who demonstrated that AuNS bioconjugated to two different antibodies selectively killed tumor cells overexpressing the targeted biomarkers when exposed to NIR laser irradiation at 80 W/cm² for 2 minutes.

In order to demonstrate a putative synergistic effect of concurrent PTT and PDT, suboptimal levels of both modalities must be determined and, as such, the results of experiments to determine optimal PDT and PTT light levels are shown in Figure 4 a and b. Employing PDT ($\lambda = 670$ nm) radiant exposures as low as 0.25 J/cm², which were clearly suboptimal (Fig. 5) in the absence of PTT, a highly significant ($P < 0.05$) decrease in cell viability was nevertheless obtained by the simultaneous application of $\lambda = 810$ nm light, that is, PTT. The synergistic effect of combined treatment (Table 1) was clearly significant with a maximum α value of 2.29 ± 0.26. The mechanism of synergism between PDT and PTT is not known in complete detail, it likely has several components. Photodynamically induced inhibition of cellular repair following sub-lethal thermal damage probably plays a role [47]. Secondly, the concerted action of both treatment modalities on cellular proteins has been proposed [48,49]. It has been shown that PDT can result in the photooxidation of intracellular enzymes such as glyceraldehyde-3-phosphate dehydrogenase and cytochrome c oxidase [50]. As a result, the enzymes undergo conformational change which, in turn, affects their susceptibility for thermal inactivation. The net effect of PDT is thus to lower the activation energy of

TABLE 1. Calculated α Values for Combined Treatment

	PTT	PTT	PTT
PDT fluence	0.5 W	14 W/cm²	28 W/cm²
0.25 J/cm²	**1.23 ± 0.14**	**2.29 ± 0.26**	0.96 ± 0.17
0.5 J/cm²	0.98 ± 0.11	**1.83 ± 0.16**	0.59 ± 0.06

α Value was calculated using the equation $(SF^a \times SF^b)/SF^{ab}$. a is PDT survival; b is PTT survival. α Values >1 convey synergistic effects, values less than 1 indicate antagonistic effects, and values equal to 1 show no or additive effects.
Bolded values signify values greater than 1, which demonstrate synergy between PDT and PTT.

protein denaturation, thus making the proteins more susceptible to thermal damage. The observation of high levels of apoptotic cell death following combined hyperthermia and PDT is consistent with this hypothesis since these proteins can be found in the mitochondrial membrane and PDT toxicity is often directed toward mitochondrial damage [24].

In the experiments reported here, the photosensitizer $AlPcS_{2a}$ was dissolved in the culture medium. Much recent work has been done to develop dual-function nano-systems consisting of gold nanomaterials conjugated with indocyanine green [34], core-shell structured up-converting nanoparticles loaded with photosesitizer [35] and gold nanorods—chlorine loaded into a chitosan-functionalized, Pluronic-based nanogel [36]. In all cell cultures treated with combined PDT + PTT in the present study the two different laser irradiations were applied simultaneously as opposed to the above mentioned experiments where either PDT was followed by PTT [36] or the reverse [35]. Although this makes direct comparison of the different results difficult, we found significant cell inhibition in the presence of NIR irradiance at PDT radiant exposures 80–100 times lower than those required for comparative results using dual-function nano-systems. This might be due to the low up-conversion luminescence emission quantum yield (<1%) and limited resonance energy transfer efficiency and the reduced availability of the photosensitizer.

Extended research efforts are presently underway to construct theranostic nanoplatforms for integrating imaging and therapy into a single system. It is clear that they will play a significant role in future cancer therapy.

ACKNOWLEDGMENTS

REFERENCES

1. Vermorken JB, Specenier P. Optimal treatment for recurrent/metastatic head and neck cancer. Ann Oncol 2010;21(7): vii252–vii261.
2. Wust P, Hildebrandt B, Sreenivasa G, Rau B, Gellermann J, Riess H, Felix R, Schlag PM. Hyperthermia in combined treatment of cancer. Lancet Oncol 2002;3(8):487–497.
3. Valdagni R, Liu FF, Kapp DS. Important prognostic factors influencing outcome of combined radiation and hyperthermia. Int J Radiat Biol Phys 1988;15:959–972.
4. Huilgol NG, Gupta S, Dixit R. Chemoradiation with hyperthermia in the treatment of head and neck cancer. Int J Hyperthermia 2010;26(1):21–25.
5. Dahl O. Mechanism of thermal enhancement of chemotherapeutic cytotoxicity. In: Urano M Douple E, editors. *Hyperthermia and oncology*. Utrecht: VSP; 1994. p 29.
6. Hopper C. Photodynamic therapy: A clinical reality in the treatment of cancer. Lancet Oncol 2000;1:212–219.
7. Brown SB, Brown EA, Walker I. The present and future role of photodynamic therapy in cancer treatment. Lancet Oncol 2004;5:497–508.
8. Green B, Cobb AR, Hopper C. Photodynamic therapy in the management of lesions of the head and neck. Br J Oral Maxillofac Surg 2013;51(4):283–287.
9. Zhou J, Wang X, Du L, Zhao L, Lei F, Ouyang W, Zhang Y, Liao Y, Tang J. Effect of hyperthermia on the apoptosis and proliferation of CaSki cells. Mol Med Rep 2011;4:187–191.
10. Gazelle GS, Goldberg SN, Solbiati L, Livraghi T. Tumor ablation with radio-frequency energy. Radiology 2000;217(3): 633–646.
11. Jolesz FA, Hynynen K. Magnetic resonance image-guided focused ultrasound surgery. Cancer J 2002;8(Suppl 1):S100–S112.
12. Huang X, El-Sayed IH, Qian W, El-Sayed MA. Cancer cell imaging and photothermal therapy in the near-infrared region by using gold nanorods. J Am Chem Soc 2006;128(6): 2115–2120.
13. Terentyuk GS, Maslyakova GN, Suleymanova LV, Khlebtsov NG, Khlebtsov BN, Akchurin GG, Maksimova IL, Tuchin VV. Laser-induced tissue hyperthermia mediated by gold nanoparticles: Toward cancer phototherapy. J Biomed Opt 2009;14:021016.
14. Gobin AM, Lee MH, Halas NJ, James WD, Drezek RA, West JL. Near-infrared resonant nanoshells for combined optical imaging and photothermal cancer therapy. Nano Lett 2007;7(7):1929–1934.
15. Dickerson EB, Dreaden EC, Huang X, El-Sayed IH, Chu H, Pushpanketh S, McDonald JF, El-Sayed MA. Gold nanorod assisted near-infrared plasmonic photothermal therapy (PPTT) of squamous cell carcinoma in mice. Cancer Lett 2008;269:57–66.
16. Kennedy LC, Bickford LR, Lewinski NA, Coughlin AJ, Hu Y, Day ES, West JL, Drezek RA. A new era for cancer treatment: Gold-nanoparticle-mediated thermal therapies. Small 2011; 7(2):169–183.
17. Oldenburg SJ, Averitt RD, Westcott SL, Halas NJ. Nano-engineering of optical resonances. Chem Phys Lett 1998;288:243–247.
18. Oldenburg SJ, Jackson JB, Westcott SL, Halas NJ. Infrared extinction properties of gold nanoshells. Appl Phys Lett 1999;75:2897–2899.
19. Huang X, Jain PK, El-Sayed IH, El-Sayed MA. Gold nanoparticles: Interesting optical properties and recent applications in cancer diagnostics and therapy. Nanomedicine 2007;2:681–693.
20. Owen MR, Byrne HM, Lewis CE. Mathematical modeling of the use of macrophages as vehicles for drug-delivery to hypoxic tumour sites. J Theor Biol 2004;226:377–391.
21. Choi MR, Stanton-Maxey KJ, Stanley JK, Levin CS, Bardhan R, Akin D, Badve S, Sturgis J, Robinson JP, Bashir R, Halas NJ, Clare SE. A cellular Trojan Horse for delivery of therapeutic nanoparticles into tumors. Nano Lett 2007; 7(12):3759–3765.
22. Valable S, Barbier EL, Bernaudin M, Roussel S, Segebarth C, Petit E, Rémy C. In vivo MRI tracking of exogenous monocytes/macrophages targeting brain tumors in a rat model of glioma. Neuroimage 2008;40(2):973–983.
23. Madsen SJ, Baek SK, Makkouk AR, Krasieva T, Hirschberg H. Macrophages as cell-based delivery systems for nanoshells in photothermal therapy. Ann Biomed Eng 2012;40(2):507–515.
24. Knowles HJ, Harris AL. Macrophages and the hypoxic tumour microenvironment. Front Biosci 2007;12:4298–4314.
25. Baek SK, Makkouk AR, Krasieva T, Sun CH, Madsen SJ, Hirschberg H. Photothermal treatment of glioma; an in vitro study of macrophage-mediated delivery of gold nanoshells. J Neurooncol 2011;104:439–448.
26. Sharman WM, Allen CM, van Lier JE. Photodynamic therapeutics: Basic principles and clinical applications. Drug Discov Today 1999;4:507–517.
27. Dolmans D, Fukumura D, Jain RK. Photodynamic therapy for cancer. Nature 2003;3:380–387.
28. Thong PSP, Ong KW, Goh NSG, Kho KW, Manivasager V, Bhuvaneswari R, Olivo M, Soo KC. Photodynamic therapy activated immune response against distant untreated lesions in recurrent angiosarcoma. Lancet Oncol 2007;8: 950–952.

29. Waldow SM, Henderson BW, Dougherty TJ. Hyperthermic potentiation of photodynamic therapy employing photofrin I and II: Comparison of results using three animal models. Lasers Surg Med 1987;7:12–22.

30. Kimel S, Svaasand LO, Hammer-Wilson M, Gottfried V, Cheng S, Svaasand E, Berns MW. Demonstration of synergistic effects of hyperthermia and photodynamic therapy using the chick chorioallantoic membrane model. Lasers Surg Med 1992;12:432–440.

31. Hirschberg H, Sun CH, Tromberg BJ, Yeh AT, Madsen SJ. Enhanced cytotoxic effects of 5-aminolevulinic acid-mediated photodynamic therapy by concurrent hyperthermia in glioma spheroids. J Neurooncol 2004;70:289–299.

32. Yanase S, Nomura J, Matsumura Y, Nagai K, Kinoshita M, Nakanishi H, Ohnishi Y, Tokuda T, Tagawa T. Enhancement of the effect of 5-aminolevulinic acid-based photodynamic therapy by simultaneous hyperthermia. Int J Oncol 2005; 27(1):193–201.

33. Kah JC, Wan RC, Wong KY, Mhaisalkar S, Sheppard CJ, Olivo M. Combinatorial treatment of photothermal therapy using gold nanoshells with conventional photodynamic therapy to improve treatment efficacy: An in vitro study. Lasers Surg Med 2008;40(8):584–589.

34. Kuo WS, Chang YT, Cho KC, Chiu KC, Lien CH, Yeh CS, Chen SJ. Gold nanomaterials conjugated with indocyanine green for dual-modality photodynamic and photothermal therapy. Biomaterials 2012;33(11):3270–3278.

35. Kim JY, Choi WI, Kim M, Tae G. Tumor-targeting nanogel that can function independently for both photodynamic and photothermal therapy and its synergy from the procedure of PDT followed by PTT. J Control Release 2013;171(2): 113–121.

36. Chen R, Wang X, Yao X, Zheng X, Wang J, Jiang X. Near-IR-triggered photothermal/photodynamic dual-modality therapy system via chitosan hybrid nanospheres. Biomaterials 2013;34(33):8314–8322.

37. Lewis CE, Pollard JW. Distinct role of macrophages in different tumor microenvironments. Cancer Res 2006;66(2): 605–612.

38. Galdiero MR, Bonavita E, Barajon I, Garlanda C, Mantovani A, Jaillon S. Tumor associated macrophages and neutrophils in cancer. Immunobiology 2013;218:1402–1410.

39. Beduneau A, Ma Z, Grotepas CB, Kabanov A, Rabinow BE, Gong N, Mosley RL, Dou H, Boska MD, Gendelman HE. Facilitated monocyte-macrophage uptake and tissue distribution of superparamagnetic iron-oxide nanoparticles. PLoS ONE 2009;4:e4343.

40. Murdcoch C, Lewis CE. Macrophage migration and gene expression in response to tumor hypoxia. Int J Cancer 2005;117:701–708.

41. Storm G, Belliot SO, Daemen T, Lasic DD. Surface modification of nanoparticles to oppose uptake by the mononuclear phagocyte system. Adv Drug Deliv Rev 1995;17:31–48.

42. Kah JC, Wong KY, Neoh KG, Song JH, Fu JW, Mhaisalkar S, Olivo M, Sheppard CJ. Critical parameters in the pegylation of gold nanoshells for biomedical applications: An in vitro macrophage study. J Drug Target 2009;17(3):181–193.

43. Yang TD, Choi W, Yoon TH, Lee KJ, Lee JS, Han SH, Lee MG, Yim HS, Choi KM, Park MW, Jung KY, Baek SK. Real-time phase-contrast imaging of photothermal treatment of head and neck squamous cell carcinoma: An *in vitro* study of macrophages as a vector for the delivery of gold nanoshells. J Biomed Opt 2012;17(12):128003.

44. Hildebrandt B, Wust P, Ahlers O, Dieing A, Sreenivasa G, Kerner T, Felix R, Riess H. The cellular and molecular basis of hyperthermia. Crit Rev Oncol Hematol 2002;43(1):33–56. Review.

45. Huang X, Jain PK, El-Sayed IH, El-Sayed MA. Determination of the minimum temperature required for selective photothermal destruction of cancer cells with the use of immunotargeted gold nanoparticles. Photochem Photobiol 2006;82:412–417.

46. Bernardi RJ, Lowery AR, Thompson PA, Blaney SM, West JL. Immunonanoshells for targeted photothermal ablation of medulloblastoma and glioma: An in vitro evaluation using human cell lines. J Neurooncol 2008;467(86):165–172.

47. Christensen T, Wahl A, Smedshammer L. Effects of haematoporphyrin derivative and light in combination with hyperthermia on cells in culture. Br J Cancer 1984;50:85–89.

48. Prinsze C, Penning LC, Dubbelman TM, VanSteveninck J. Interaction of photodynamic treatment and either hyperthermia or ionizing radiation and of ionizing radiation and hyperthermia with respect to cell killing of L929 fibroblasts, Chinese hamster ovary cells and T24 human bladder carcinoma cells. Cancer Res 1992;52:117–120.

49. Rasch MH, Tijssen K, VanSteveninck J, Dubbelman TM. Synergistic interaction of photodynamic treatment with the sensitizer aluminum phthalocyanine and hyperthermia on loss of clonogenicity of CHO cells. Photochem Photobiol 1996;64:586–593.

50. Prinsze C, Dubbelman TM, VanSteveninck J. Potentiation of the thermal inactivation of glyceraldehydes-3-phosphate dehydrogenase by photodynamic treatment. A possible model for the synergistic interaction between photodynamic therapy and hyperthermia. Biochem J 1991;276:357–362.